Int. J. Heat Mass Transfer. Vol. 10, pp. 349–359. Pergamon Press Ltd. 1967. Printed in Great Britain

THE INFLUENCE OF MASS TRANSFER ON LIQUID FILM BREAKDOWN

A. B. PONTER, G. A. DAVIES, T. K. ROSS and P. G. THORNLEY

Department of Chemical Engineering, University of Manchester Institute of Science and Technology, Manchester, 1

(*Received* 30 *May* 1966 *and in revised form* 9 *September* 1966)

Abstract—A model is presented to account for breakdown of a vertical laminar liquid film exposed to a soluble countercurrent gas stream. The conditions under which a stable dry patch is first formed may be predicted from the equation

$$\frac{\Gamma}{\mu} = 1{\cdot}12(1 - \cos\theta)^{0{\cdot}6}\left(\frac{\rho\gamma_e^3}{\mu^4 g}\right)^{0{\cdot}2}.$$

Experimental wetting rate values are reported for water and ethanol–water films on vertical copper, stainless steel, Perspex and carbon surfaces. The effect of different tube lengths and surface roughnesses are investigated for a temperature range 20°–50°C during absorption of ethanol–air mixtures into the films. Effective surface tensions and contact angles under mass-transfer conditions are measured and correlated with values derived from a sessile-drop method. The predicted and measured values of wetting rates producing stable patches are in close agreement for all surfaces.

NOMENCLATURE

M = mass T = time L = length t = temp.

- a_0, mean film thickness in wave flow (L);
- g, gravitation constant (LT^{-2});
- h, height (L);
- h_b, heat-transfer coefficient ($MT^{-3}t^{-1}$);
- m, mean film thickness in laminar flow (L);
- q, peripheral volumetric flow rate (L^2T^{-1});
- u, velocity (LT^{-1});
- x, y, z, Cartesian co-ordinates.

Greek symbols

- Γ, peripheral mass flow rate ($ML^{-1}T^{-1}$);
- γ, surface tension (MT^{-2});
- γ_e, effective surface tension (MT^{-2});
- $\Delta\gamma$, surface tension difference (MT^{-2});
- θ, contact angle (dimensionless);
- λ, wavelength (L);
- μ, viscosity ($ML^{-1}T^{-2}$);
- ρ, density (ML^{-3}).

Subscripts

- L, liquid;
- V, vapour.

THE INFLUENCE OF MASS TRANSFER ON LIQUID FILM BREAKDOWN

A SUCCESSFUL gas–liquid contacting device must distribute liquid as a thin film providing the maximum surface area to a countercurrent gas stream. Low efficiencies in distillation and absorption towers have been attributed to film breakdown resulting in reduced transfer surface areas [1, 2].

The flow properties of falling films have been extensively studied both theoretically and experimentally. Recent investigations have been focused on wave formation and growth in liquids as these phenomena contribute appreciably to increases in heat- and mass-transfer rates. No comparable study has been made to investigate the mechanism of film rupture produced by gas absorption or temperature gradients in the liquid.

Film breakdown caused by temperature gradients

Shires [3], Hallett [4], Hsu [5] and Murgatroyd [6] have examined the role of heat transfer causing breakdown of the liquid film into channels. Shires investigated liquid film breakdown during the cooling of electrically-heated

rods. Four regimes of film behaviour with increasing rod temperature were described, progressive evaporation, dry patch formation, flooding and sputtering. No quantitative assessments were made. Hallett studied the breakdown of a water film on a 6-ft length of vertical heated copper tube. It was assumed that breakdown was a function of surface tension difference forces set up due to uneven heating caused by the wave flow pattern. The results were correlated by the equation

$$0{\cdot}0058\left(\frac{h_b}{1000}\right)^{6{\cdot}89}\left(\frac{\lambda}{a_0}\right)\left(\frac{\Delta\gamma}{\gamma}\right)=\left(\frac{4\rho q}{\mu}\right)^{-0{\cdot}68} \quad (1)$$

The term $\Delta\gamma/\gamma$ defines the maximum available energy for work that can be utilized to distort and rupture the film. However, λ/a_0 defined by Kapitsa [8] has been shown by Stainthorp and Allen [7] to be a significant parameter at low flow rates only ($Re < 50$) and over the flow range under investigation (Re 130–1400) a complicated flow pattern exists, thus making it unlikely that λ/a_0 has any physical significance. Hsu observed the effect of heating thin liquid films on the inside of a glass tube surrounded by a stagnant air space. It was suggested that the mechanism of film breakdown was dependent on the thermal boundary layer formed as the wavy liquid film proceeded down the heated tube. In order that a surface tension difference should occur at adjacent points on the surface it is necessary that this layer should penetrate it. If the gas interface is strongly turbulent, the temperature variation is short-lived and the surface disturbance is random without the formation of dry spots. Should a steady temperature variation exist for long enough a dry spot will form provided sufficient heat is supplied. There was a critical mean film thickness for dry patch formation which to be stable had to be less than the peak wave thickness of the liquid approaching the dry spot. Hartley and Murgatroyd [9] presented a theoretical treatment of the break-up of thin liquid layers flowing isothermally over solid surfaces which Murgatroyd developed to include shear and form forces produced by a countercurrent gas stream. Experimental results of film breakdown due to heat transfer from the solid surface were then used to show the predominance of these forces. In an analogous situation for mass transfer, Bond and Donald [10] found practically no increase in the minimum wetting rate, that is, the film thickness remained constant when the gas velocity was increased from 2 to 8 ft/s for ammonia gas absorbed on a water film, although this increase would have a marked influence on the shear and form forces.

Film breakdown caused by mass transfer

Over the last 30 years workers have reported the phenomenon of film breakdown when observing liquid flow in packed absorption and distillation columns [1]. No mechanism has been elucidated, but attempts at explanation have been forwarded in terms of surface tension and surface tension differences caused by mass transfer into the liquid film. Norman and Binns [11] gave results for breakdown produced by the absorption of ethanol vapour in a water stream flowing down a glass wetted wall column. These results were correlated by the equation

$$\frac{3q\mu}{\rho g}=1{\cdot}2\times10^{-6}-1{\cdot}76\times10^{-8}\,\gamma\Delta\gamma. \quad (2)$$

$\Delta\gamma$ was defined as the difference between the bulk and equilibrium surface tensions. Using $\Delta\gamma$ as a driving force, and assuming that the contact angle between the liquid and solid surface at breakdown under mass-transfer conditions was constant, Ponter and Thornley [12] correlated the results of ethyl alcohol–air mixtures on glass surfaces together with the data of Norman and Binns for copper surfaces, by equating the momentum change bringing the film to rest with the surface tension forces.

Thus

$$\frac{\Gamma}{\mu}=0{\cdot}90\left(\frac{\rho\,\Delta\gamma^3}{\mu^4 g}\right)^{0{\cdot}2} \text{ for a copper surface} \quad (3)$$

$$\frac{\Gamma}{\mu}=0{\cdot}96\left(\frac{\rho\,\Delta\gamma^3}{\mu^4 g}\right)^{0{\cdot}2} \text{ for a glass surface.} \quad (4)$$

MODEL

A model is now developed to predict liquid film breakdown in the presence of mass transfer. Determinations of film breakdown using a wide range of tube materials and experimental conditions were made to test the validity of the model.

Consider a film of liquid flowing over a vertical surface. This is illustrated in Fig. 1 where a uniform laminar stream with mean velocity u flows over a vertical surface ABDE. Consider the forces acting in the yz-plane through CY which is shown in cross-section (Fig. 1). If the dry patch is stable the surface

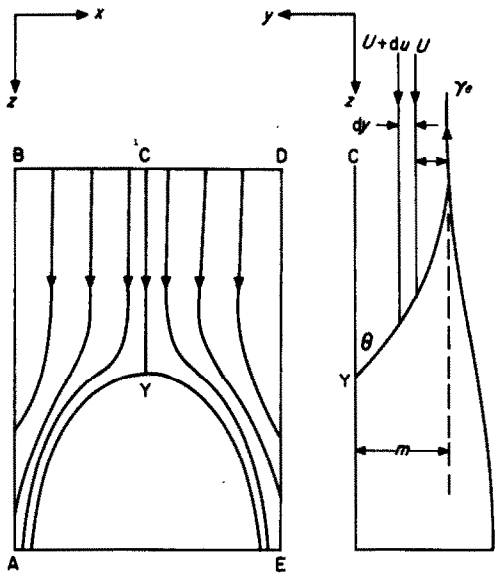

FIG. 1. Film breakdown in falling liquid film showing "dry patch" formation.

tension forces along YC must balance the fluid force brought about by the loss in momentum in bringing the liquid to rest at point Y. This is

$$\int_0^m \rho u^2 \, dy = \gamma_e(1 - \cos\theta) \qquad (5)$$

where u, the axial velocity is a function of y,

$u = f(y)$;

γ_e is the effective surface tension; and

θ is the corresponding contact angle.

The solution of this equation depends on the velocity profile assumed.

Considering the condition of steady laminar flow without surface waves, the Navier–Stokes equation reduces to the well-known Nusselt solution [13]

$$u = \frac{\rho g}{2\mu}(m^2 - y^2) \qquad (6)$$

and the volume of liquid q flowing per unit time through a film of unit width will be given by

$$\int_0^m u \, dy = \frac{\rho g m^3}{3\mu}. \qquad (7)$$

Thus for a given mass flow rate Γ,

$$\text{the film thickness } m = \left(\frac{3\mu\Gamma}{\rho^2 g}\right)^{\frac{1}{3}}. \qquad (8)$$

Substitution of equation (6) into the model gives

$$\int_0^m \frac{\rho^3 g^2}{4\mu^2}(m^2 - y^2)^2 \, dy = \gamma_e(1 - \cos\theta) \qquad (9)$$

and

$$\frac{2\rho^3 g^2 m^5}{15\mu^2} = \gamma_e(1 - \cos\theta). \qquad (10)$$

Hence

$$\frac{\Gamma}{\mu} = 1{\cdot}116\,(1 - \cos\theta)^{0{\cdot}6}\left(\frac{\rho\gamma_e^3}{\mu^4 g}\right)^{\frac{1}{3}}. \qquad (11)$$

To test the validity of the model, the two parameters θ, the contact angle of the liquid to the vertical solid surface under "through flow" conditions and γ_e, the effective surface tension measured in an absorbing environment must be evaluated.

APPARATUS

Details of the liquid flow system are given in Fig. 2. Specimen tubes of copper, stainless steel, Perspex and fine grade carbon were carefully pretreated by polishing to known surface roughness, measured by a Talysurf meter, degreasing

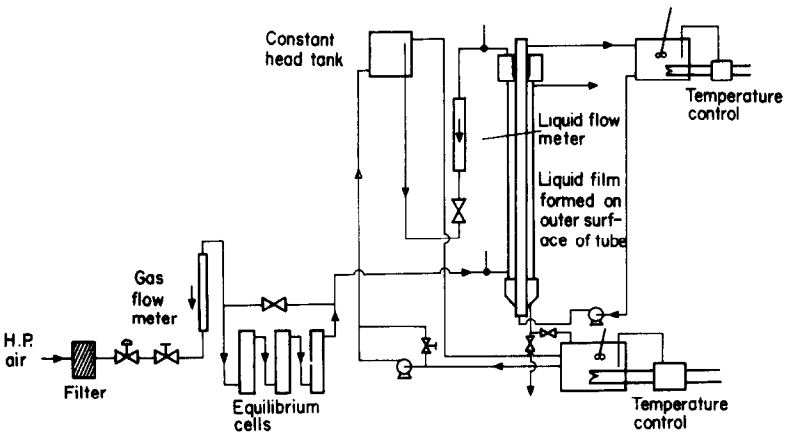

FIG. 2. Diagram of apparatus.

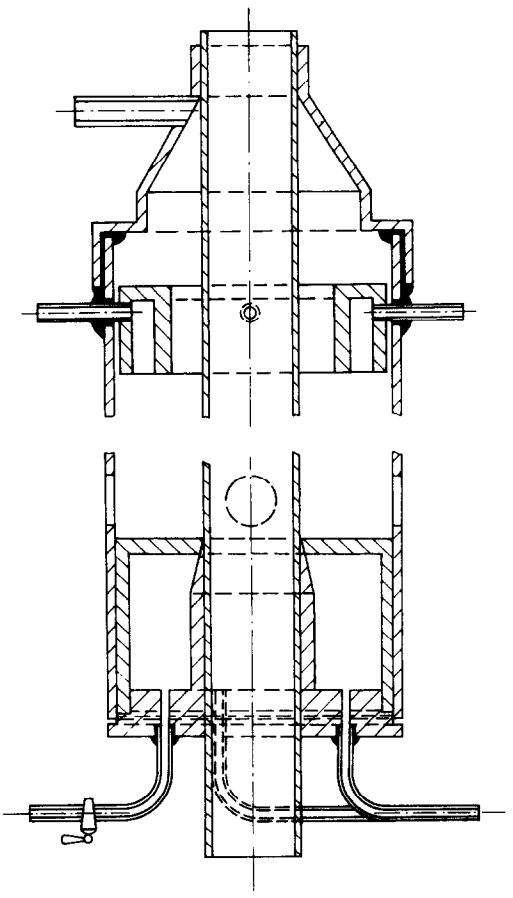

FIG. 3. The distributor and catchpot.

and washing in distilled water for several hours before being assembled under controlled conditions. Distilled water was then allowed to flow down the tube for a week before results were taken.

For good liquid distribution around the column, a simple weir-type distributor or Aerox ring had been found to be effective at very low flow rates for liquids wetting the inside of a tube. The distributor designed and shown in Fig. 3 was developed to give uniform flow for higher flow rates with liquid flow over the tube exterior. The annulus width was set by calculating the corresponding film thickness from Nusselt's equation to prevent surging from the distributor. The vent tap allowed entrained air to escape before start-up. A line diagram of the vapour flow system is given in Fig. 2. The compressed air drawn from the mains was previously filtered to eliminate any entrained oil droplets from the compressor unit, before passing through two reducing valves, then metered through a glass Rotameter. The air then passed through a series of equilibrium cells containing at a controlled temperature, pure ethanol before flowing countercurrent to the liquid film. The vertical alignment of the tube was checked optically.

Studies of the effect of tube alignment have

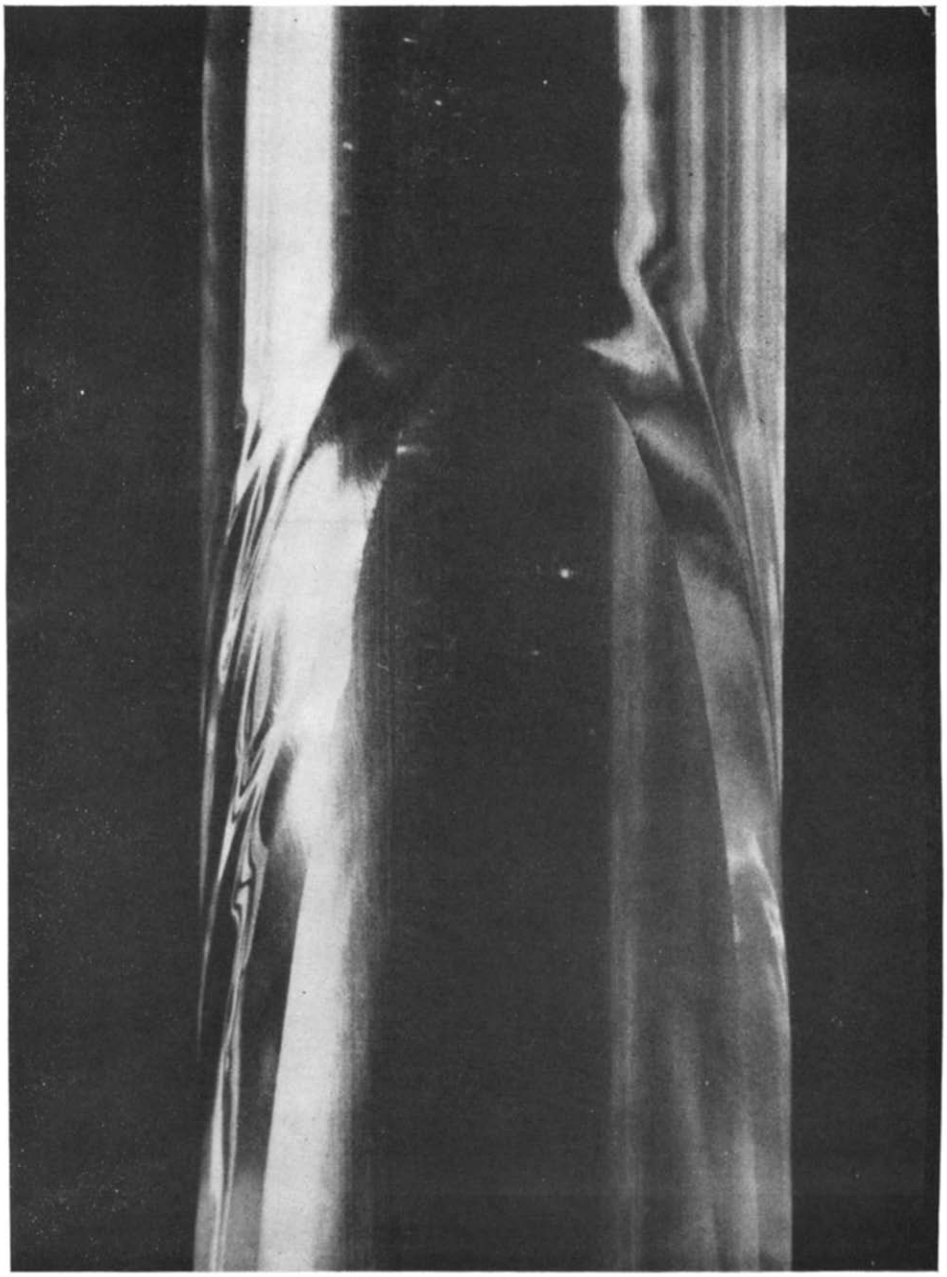

FIG. 4(a). Photograph illustrating film breakdown and formation of a stable patch.

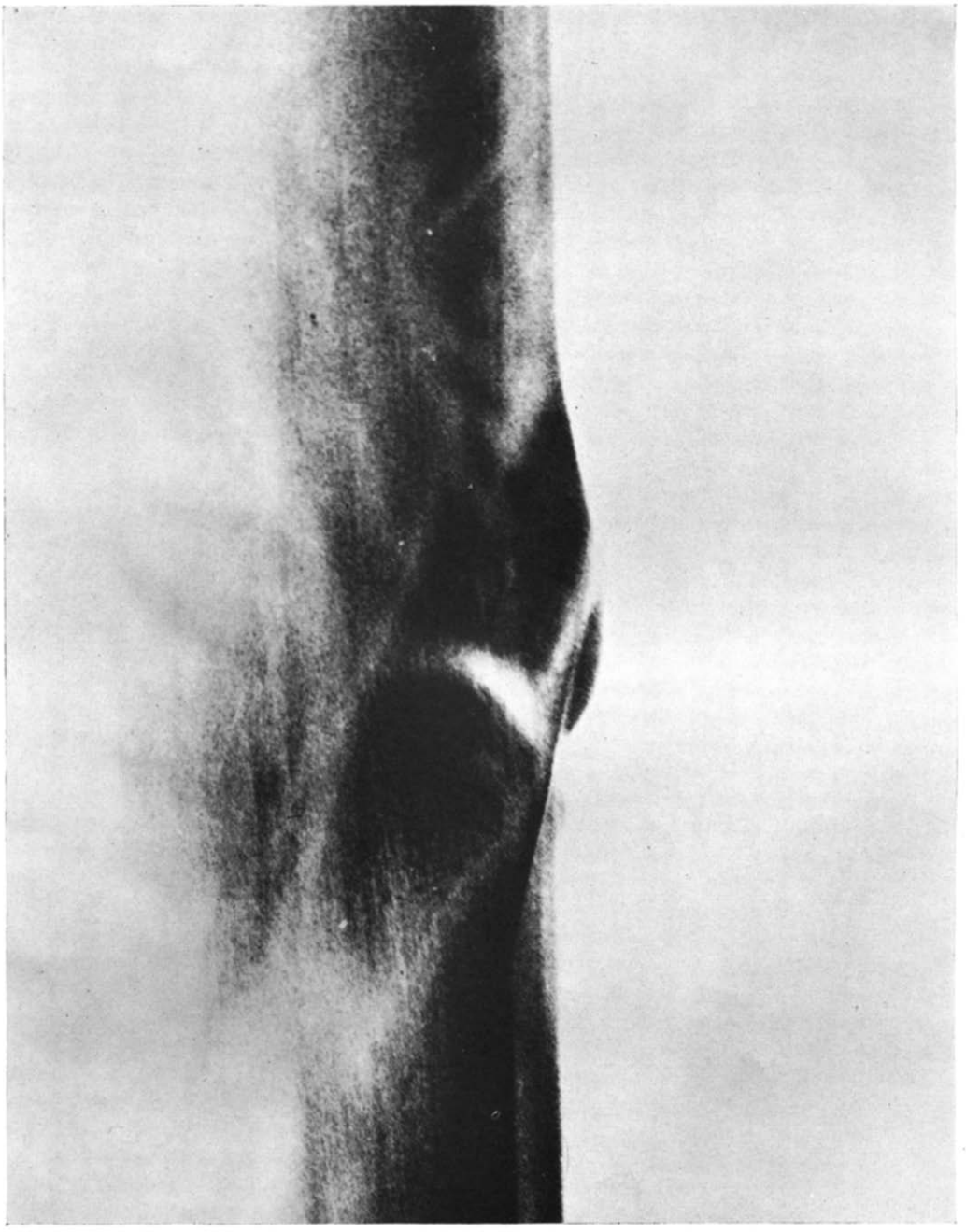

FIG 4(b). Photograph illustrating liquid film breakdown and formation of a stable dry patch.

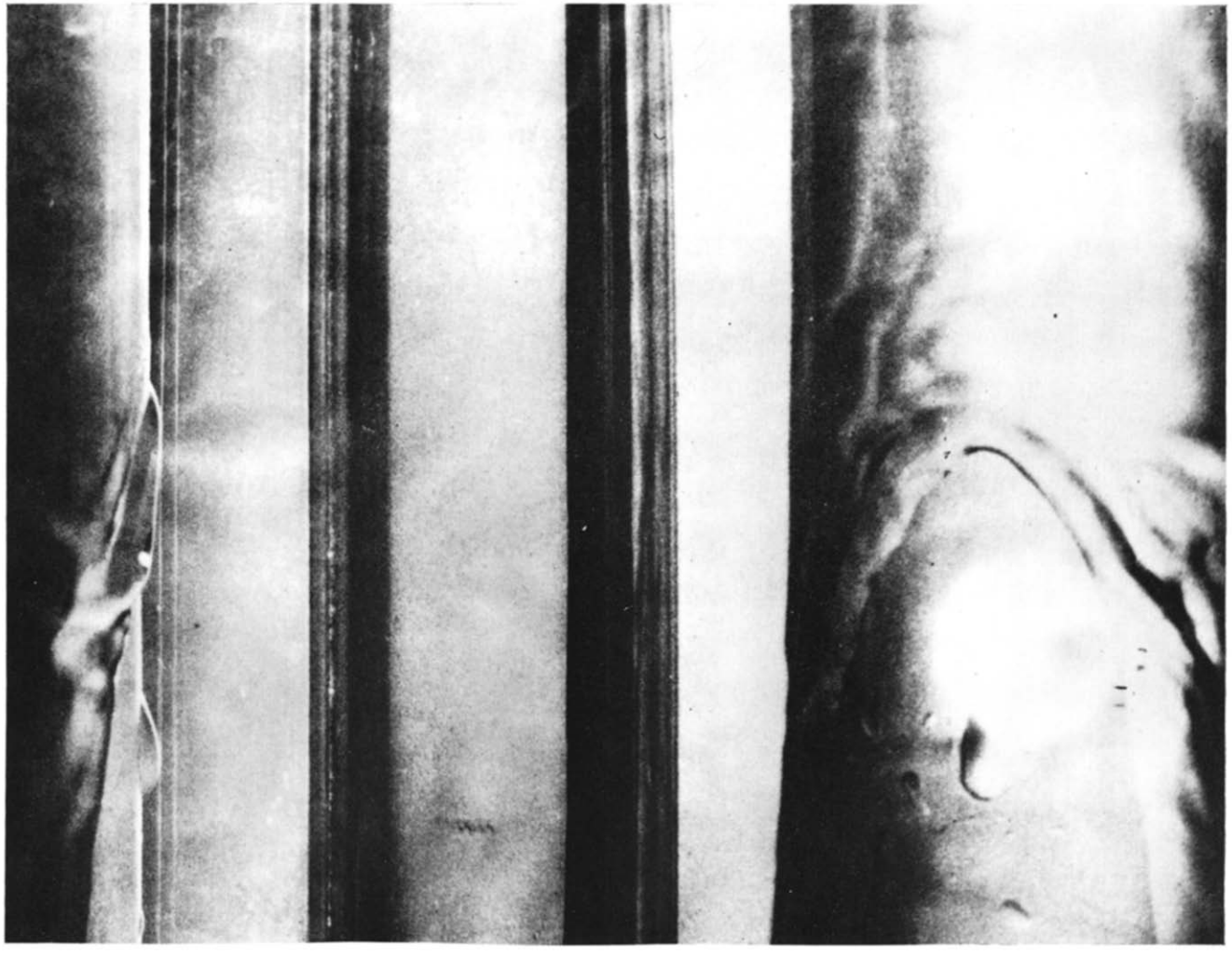

FIG. 5. Breakdown of a water film on a 30-cm roughened Perspex tube during absorption. Water flow rate 1·15 g/cm s at 20°C.

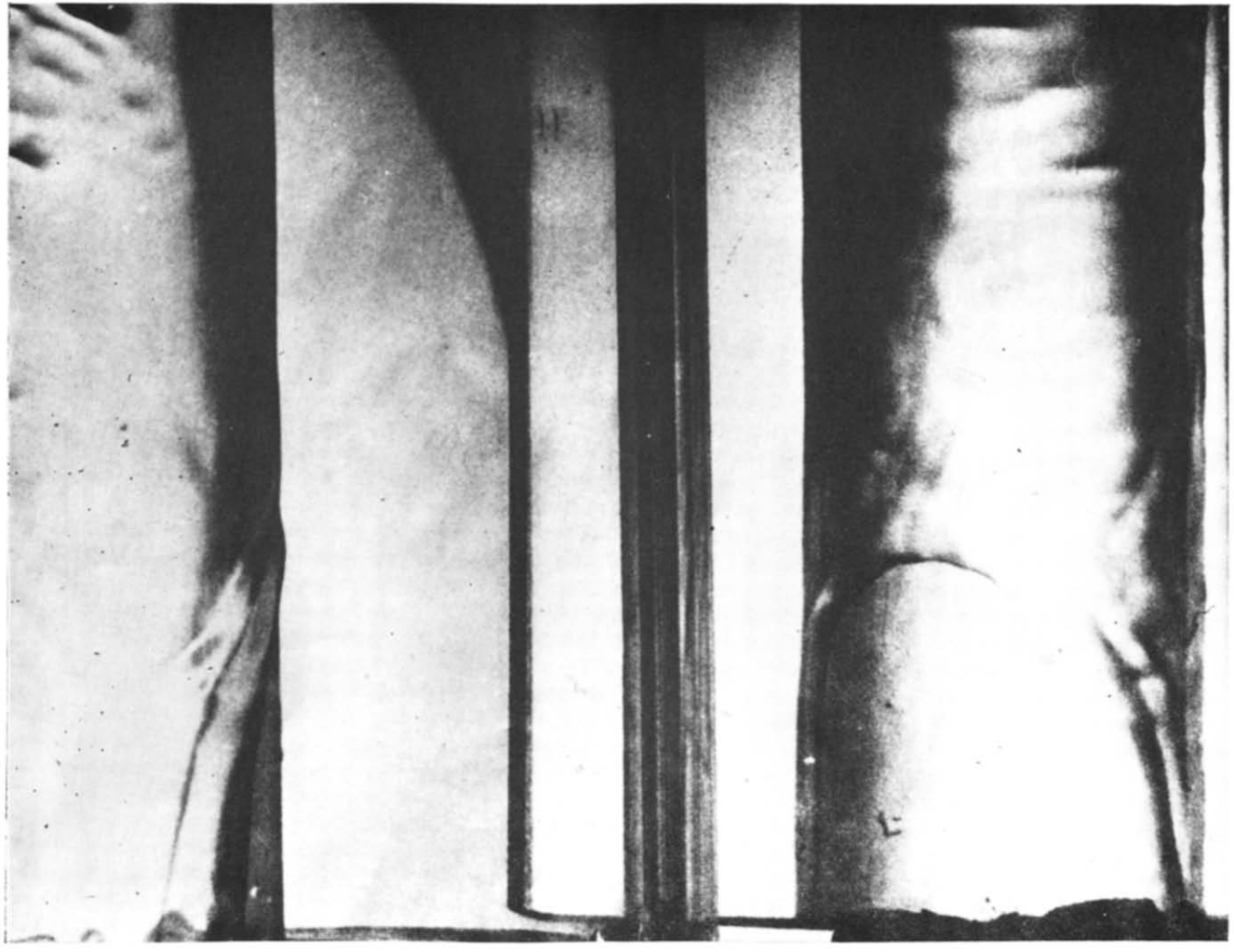

FIG. 6. Breakdown of a water film on a 120-cm roughened Perspex tube during absorption of ethanol.

shown that for an inclination of less than 8′ no effect on hydrodynamic properties ensues but above this value large variations are produced.

Reduction of the liquid flow rate resulted in the breakdown of the liquid film into rivulets and the formation of dry patches at the bottom of the tube. Initially these dry patches were recovered by liquid almost immediately and were quite unstable. Further reduction of the liquid flow rate resulted in the formation of a stable dry patch and this was taken as the minimum wetting rate. The ethanol vapour stream was shut off immediately afterwards so as to expose the tube surface to the gas for as short a time as possible. The tube immediately became completely rewetted, and the surface was irrigated with water for a day before another experiment was carried out.

This procedure was repeated at different temperatures for water and ethanol–water films.

MEASUREMENT OF CONTACT ANGLE

Figures 4(a) and 4(b) illustrate the formation of a stable dry patch when the liquid flow rate has been reduced to the final minimum wetting rate. The formation of a collar of liquid around the top of the dry patch completely eclipsed the point of contact of liquid to the vertical solid surface and thus prevented a direct estimation of contact angle photographically.

An attempt was made to overcome this difficulty by mounting a mirror at 45° to the plane of view in order to observe the dry patch simultaneously from two positions at right angles. This was only partially successful because the mirror could not be placed close enough to the column on account of the outside glass tube. Thus a large depth of focus was required and the camera had to be mounted far from the subject magnifying any errors involved in the positioning of the mirror. Successful measurements were made as illustrated in Figs. 5 and 6 when using a Perspex tube. Here an intense light source was not used to directly illuminate the tube surface but was placed at the tube end and all light rays not travelling through the Perspex annulus were effectively shielded. The gas–liquid interface was clearly defined and photographed at right angles to the liquid surface. This method has been further developed and will be the subject of a future communication.

These values of dynamic contact angles obtained on Perspex tubes were compared with values measured from a sessile drop on a horizontal Perspex surface of the same roughness under the same environmental conditions and were found to be in close agreement (Fig. 7).

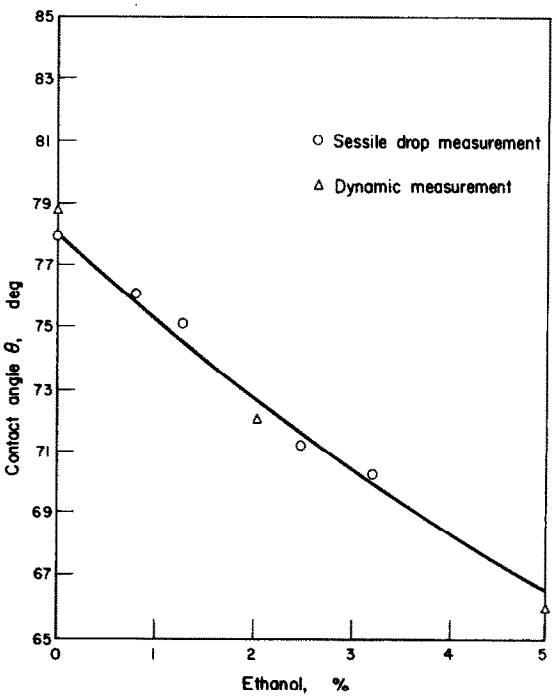

FIG. 7. Contact angle of ethanol–water mixtures measured in air on smooth Perspex at 20°C.

Since the optical method described could only be used for translucent materials, the values of contact angle measured from sessile drop determinations were taken for the metal and carbon surfaces.

The sessile drop measurements

A comparison was first made between the

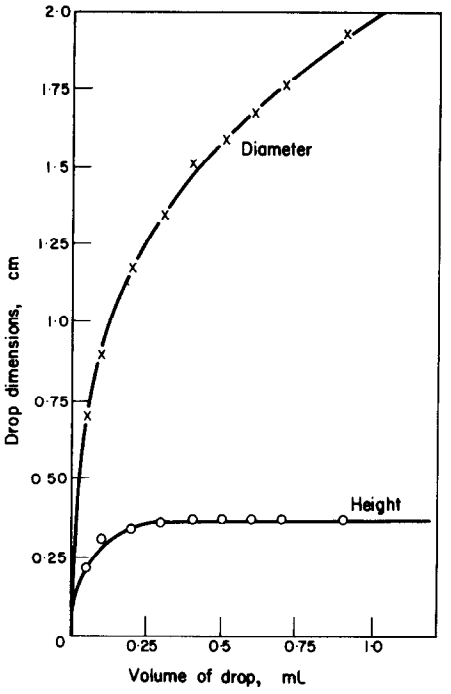

FIG. 8(a). Sessile drop of water in air on smooth copper (20°C).

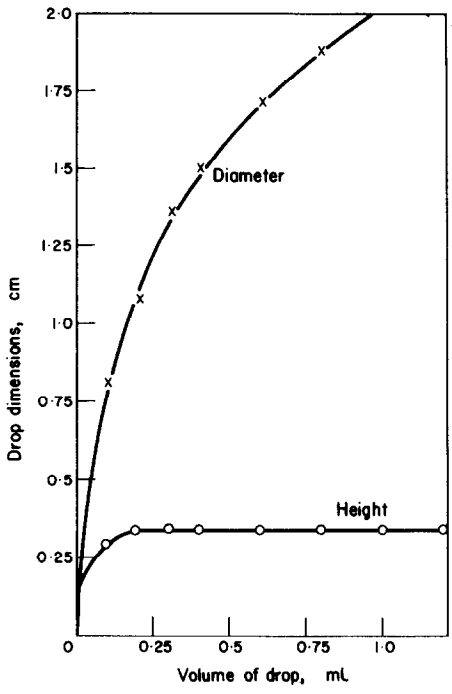

FIG. 8(c). Sessile drop of water in air on smooth Perspex (20°C).

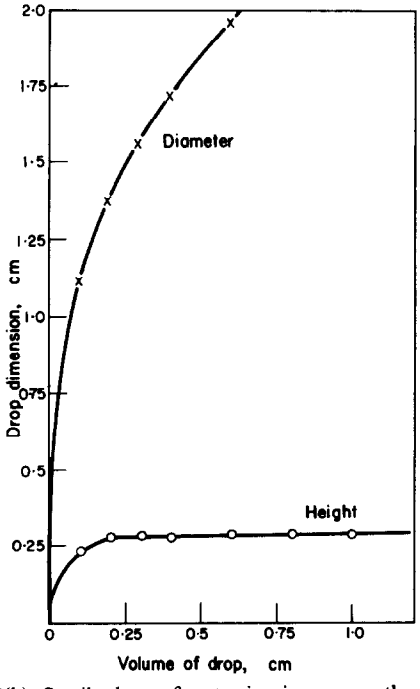

FIG. 8(b). Sessile drop of water in air on smooth stainless steel (20°C).

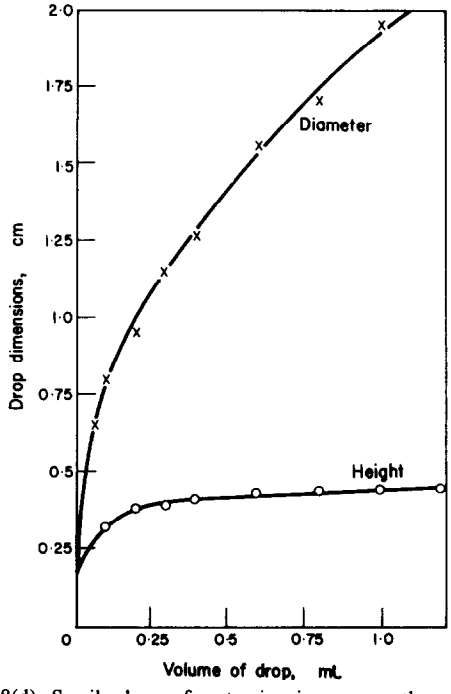

FIG. 8(d). Sessile drop of water in air on smooth carbon (20°C).

contact angle measured directly by a goniometer eyepiece of a travelling microscope with the contact angle calculated from the equilibrium drop height and the physical properties of the liquid. The equation derived by Padday [14] had been shown to be accurate when the drop size was sufficiently large.

$$1 - \cos\theta = \frac{\rho g h^2}{2\gamma_{LV}} \qquad (12)$$

where h is the measured equilibrium drop height.

Figures 8(a)–8(d) show the effect of increasing drop volume upon the dimensions of the drop using distilled water upon surfaces of copper, stainless steel, Perspex and carbon. In each case the roughness of the solid sample had been prepared to 15–25 $\times$ 10^{-6} cm and the sample stored over silica gel. The increase in the diameter of the drop with volume is included to show the uniformity of spreading of the drop and the retention of the circular shape. For copper, stainless steel and Perspex the equilibrium height of the drop was reached when the volume exceeded 0·5–0·6 ml and for carbon when the volume exceeded 0·8 ml. The contact angle measured by the goniometer was constant above volumes of 0·2 ml for copper, stainless steel and Perspex and 0·6 for carbon.

A comparison of the equilibrium contact angles for water in air for the studied surfaces at 20°C is given in Table 1.

Measurements of contact angle of water drops were made on the four surfaces. In each case the volume of the water drops was greater than the critical volume defined by Padday. Each surface was carefully prepared by polishing, degreasing and finally washing in distilled water to a standard surface roughness measured by a Talysurf meter, at 20°C, of 15–25 $\times$ 10^{-6} cm and 130–150 $\times$ 10^{-6} cm. The specimens were stored over silica gel for a period of 24h before use. Results are shown in Figs. 9(a)–9(d). The effect of surface roughness has been described elsewhere by Ponter and Thornley [15]. These experiments were repeated in the presence of

Table 1. A comparison of the observed and theoretical values of the equilibrium contact angles of distilled water in air on various surfaces, at 20°C

Surface	Contact angle: By goniometer	Contact angle: By equilibrium height
Copper	87°	87°
Stainless steel	66°	64°
Perspex	79°	78°
Carbon	102°	107°

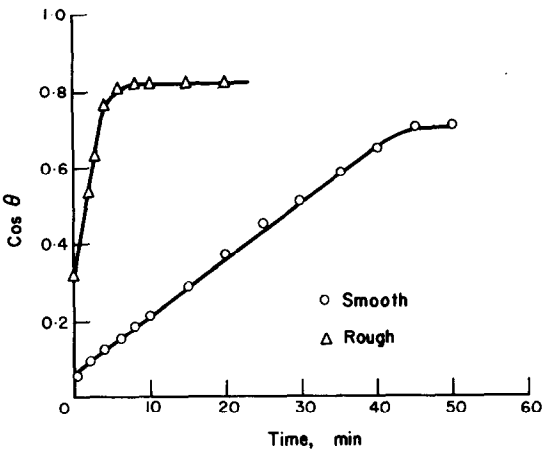

FIG. 9(a). Variation of contact angle of water on copper in the presence of saturated ethanol–air mixtures at 20°C.

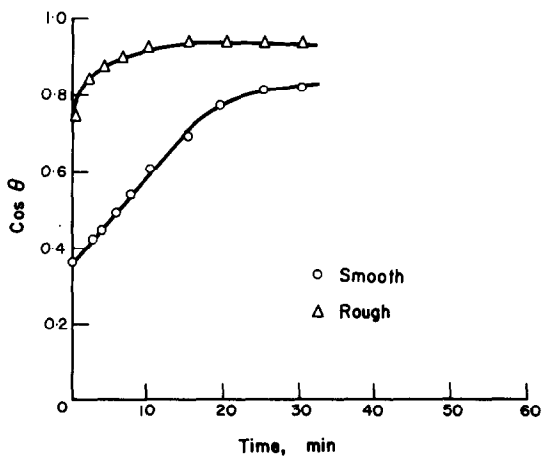

FIG. 9(b). Variation of contact angle of water on stainless steel in the presence of saturated ethanol–air mixture at 20°C.

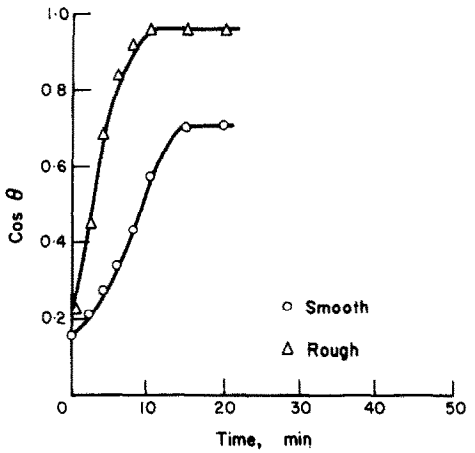

FIG. 9(c). Variation of contact angle of water on Perspex in the presence of saturated ethanol–air mixture at 20°C.

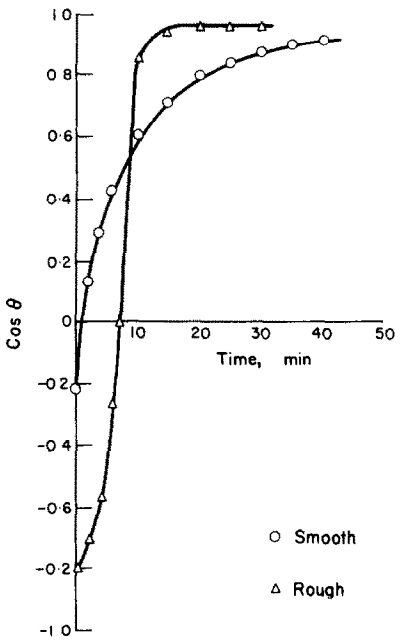

FIG. 9(d). Variation of contact angle of water on graphite in the presence of saturated ethanol–air mixture at 20°C.

ethanol vapour. In this case the drops spread slowly across the surface until an equilibrium position had been reached. The spreading can be attributed to adsorption of ethanol vapour directly onto the solid surface and absorption of ethanol into the droplet, causing a reduction in the surface tension.

We have shown [16] that previous adsorption of ethanol onto a clean copper surface reduces the initial contact angle by up to 17 per cent of the equilibrium value.

Measurements of surface tension

The surface tension of the liquid film changes during absorption. At the point of breakdown, absorption into the liquid is taking place and also adsorption of vapour onto the freshly exposed surface. The value of the surface tension under these conditions is required in the model. To simulate this the surface tension of water and water–alcohol mixtures were measured in an environment of various alcohol–air mixtures for a range of contact times. Two methods were considered.

(a) using the de Nouy balance. Results are given in Fig. 10. The prime disadvantage with this method is the effect of ring movement during withdrawal which induces mixing at the gas–liquid interface.

(b) the Pendant drop method [17]. Results are shown in Fig. 10. For low alcohol concentrations in air and at low contact times the results from this method are reliable. However, with increasing concentrations interfacial instability takes place induced by concentration gradients near the interface which causes "kicking" and thus mixing in the drop.

Figures 11(a)–11(c) show the effect of temperature and tube length on minimum flow rate to sustain a stable dry patch. It can be seen that in every case the minimum flow rate decreases with increasing temperature. Since the density, surface tension and viscosity decrease with increasing temperature, values of the minimum flow rate calculated from equation (11) will likewise decrease. However, at the higher temperatures, above 40°C, the value predicted from the model is higher than the observed values. This is probably due to the effect of evaporation from the film and at these temperatures the gas

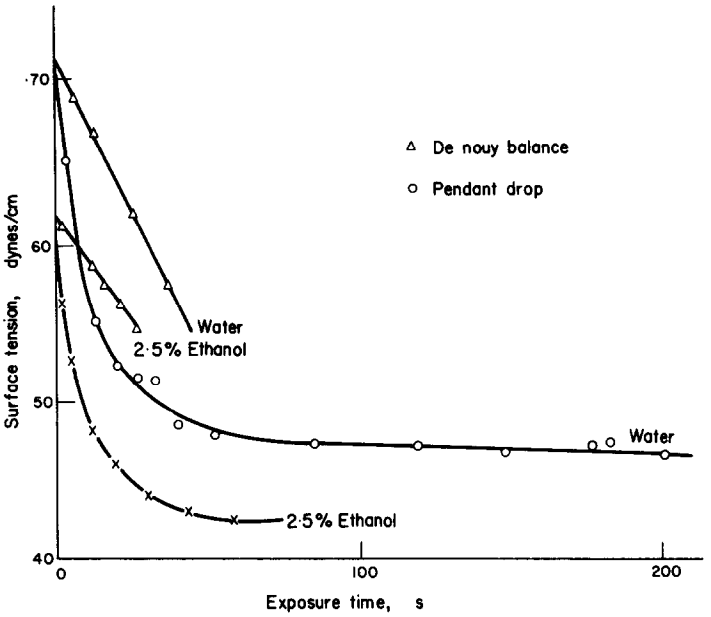

FIG. 10. Changes in surface tension of water and water–ethanol mixtures in contact with air saturated with ethanol at 20°C.

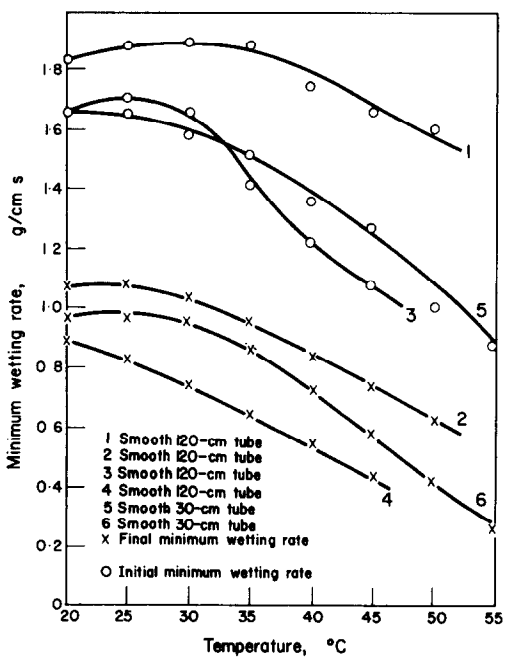

FIG. 11(a). The minimum wetting rates of water on copper tubes.

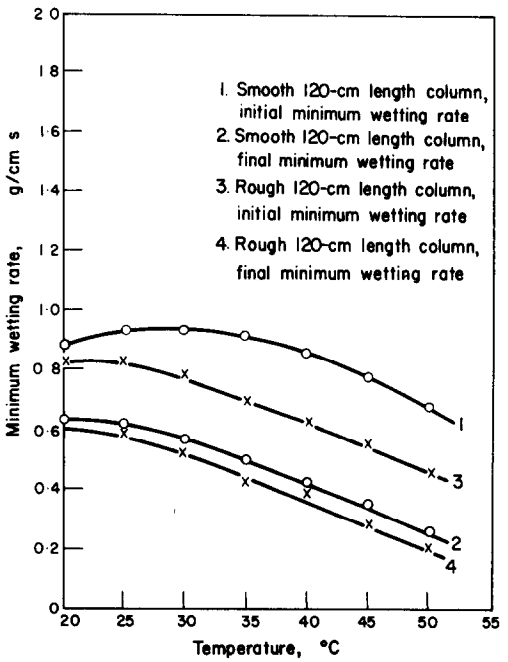

FIG. 11(b). The minimum wetting rates of water on stainless-steel tubes.

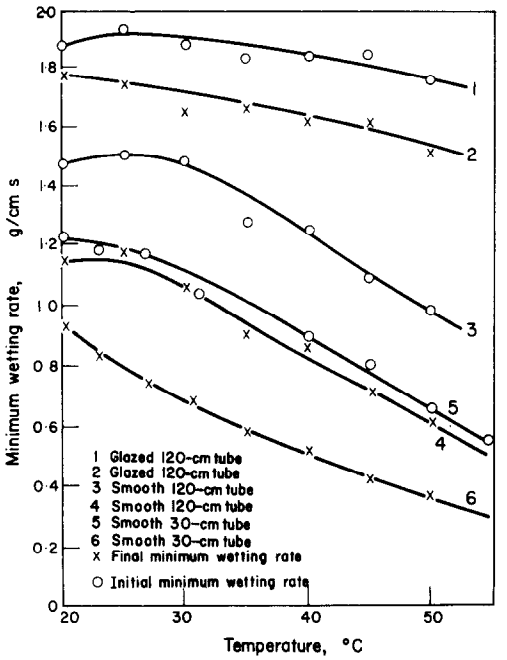

FIG. 11(c). The minimum wetting rates of water on Perspex tubes.

was not in thermal equilibrium with the liquid.

The effect of surface roughness in stabilizing the film (Fig. 11) can be predicted from the results of experiments on flat plates which showed improvement in wetting as the surface roughness increased.

Validity of the model

Equation (11) defines the minimum liquid flow rate to sustain a stable dry patch. Experimental results for water films in the presence of a saturated alcohol–air mixture are shown in Table 2. Comparison of these values with the values predicted by equation (11) shows good agreement on all the different surfaces studied.

CONCLUSIONS

It has been demonstrated that the equation:

$$\frac{\Gamma}{\mu} = 1{\cdot}12(1 - \cos\theta)^{0{\cdot}6}\left(\frac{\rho\gamma_e^3}{\mu^4 g}\right)^{0{\cdot}2}$$

can be used to interpret the mechanism of film breakdown under conditions of mass transfer. The analogy between this and the corresponding situation where heat transfer takes place would suggest that a similar mechanism is involved. Therefore contact angle and surface tension under evaporative conditions must be measured before any theoretical prediction can be made.

REFERENCES

1. W. S. NORMAN, *Absorption, Distillation and Cooling Towers*. Longmans (1961).
2. H. L. SHULMAN, C. F. ULLRICH, A. Z. PROULX and J. O. ZIMMERMAN, *A.I.Ch.E.Jl.* **1**, 253 (1955).
3. G. L. SHIRES, A. R. PICKERING and P. T. BLACKER, Film cooling of vertical fuel rods, *A.E.E.W. Rep.* 343 (1964).
4. V. A. HALLETT, *Int. J. Heat Mass Transfer* **9**, 283 (1966).
5. Y. Y. HSU, *A.I.Ch.E. 51st National Meeting*, Puerto Rico (1965).
6. W. MURGATROYD, *Int. J. Heat Mass Transfer* **8**, 297 (1965).
7. F. P. STAINTHORP and J. M. ALLEN, *Trans. Instn Chem. Engrs* **43**, 85 (1965).
8. P. C. KAPITSA, *Zh. Eksp. Teor. Fiz.* **18**, 19 (1948).
9. D. E. HARTLEY and W. MURGATROYD, *Int. J. Heat Mass Transfer* **7**, 1003 (1964).

Table 2. A comparison of the observed and predicted minimum wetting rates for each column

Surface	Surface roughness (cm)	Temperature (°C)	System	Tube length	Observed minimum wetting rate	Predicted final minimum wetting rate
Copper	$15–25 \times 10^{-6}$	20	Ethanol–water	120 cm column	0·974 g/s cm	0·910 g/s cm
	$15–25 \times 10^{-6}$	20	Ethanol–water	30 cm column	0·880 g/s cm	0·910 g/s cm
Stainless steel	$15–25 \times 10^{-6}$	20	Ethanol–water	120 cm column	0·555 g/s cm	0·674 g/s cm
Perspex	$15–25 \times 10^{-6}$	20	Ethanol–water	120 cm column	1·145 g/s cm	0·810 g/s cm
	$15–25 \times 10^{-6}$	20	Ethanol–water	30 cm column	0·935 g/s cm	0·810 g/s cm
Carbon	$15–25 \times 10^{-6}$	20	Ethanol–water	30 cm column	0·943 g/s cm	1·037 g/s cm

10. J. BOND and M. B. DONALD, *Chem. Engng. Sci.* **6**, 238 (1956).
11. W. S. NORMAN and D. T. BINNS, *Trans. Instn Chem. Engrs* **28**, 294 (1960).
12. A. B. PONTER and P. G. THORNLEY, *Chem. Process Engng* 402 (1964).
13. W. NUSSELT, *Z. Ver. Dt. Ing. Forsch.* **54**, 1154 (1910).
14. J. F. PADDAY, *2nd Int. Cong. of Surface Activity*, **3**, 136 (1956).
15. A. B. PONTER and P. G. THORNLEY, *Nature, Lond.* **207**, 1288 (1965).
16. A. B. PONTER, G. A. DAVIES and P. G. THORNLEY, *Can. J. Chem. Engng* **44**, 178 (1966).
17. S. FORDHAM, *Proc. R. Soc.* **A 194**, 1 (1948).

Résumé—On présente un modèle pour expliquer la rupture d'un film liquide vertical laminaire en contact avec un écoulement à contrecourant d'un gaz soluble. Les conditions sous lesquelles une tache sèche stable se forme pour la première fois peuvent être prévues à partir de l'équation:

$$\frac{\Gamma}{\mu} = 1{,}21(1 - \cos\theta)^{0.6}\left(\frac{\rho\gamma_e^3}{\mu^4 g}\right)^{0.2}.$$

On donne les valeurs expérimentales de la vitesse de mouillage pour des films d'eau et de mélange eau et éthanol sur des surfaces verticales de cuivre, d'acier inoxydable, de Perspex et de carbone. On a étudié l'effet de différentes longueurs de tube et de rugosités de surface pour une gamme de températures de 20° à 50°C pendant l'absorption de mélanges d'air et d'éthanol dans les films. Les tensions superficielles effectives et les angles de contact dans les conditions du transport de masse sont mesurés et comparés avec les valeurs obtenues grâce à la méthode de la goutte pendante. Les valeurs prévues et mesurées des vitesses de mouillage produisant des taches stables sont en excellent accord pour toutes les surfaces.

Zusammenfassung—Es wird ein Modell angegeben für das Aufreissen eines senkrechten laminaren Flüssigkeitsfilms, der einem im Gegensinn strömenden löslichen Gas ausgesetzt ist. Die Bedingungen unter welchen sich eine stabile Trockenzone bildet, entsprechen folgender Gleichung.

$$\frac{\Gamma}{\mu} = 1{,}12(1 - \cos\theta)^{0.6}\left(\frac{\rho\gamma_e^3}{\mu^4 g}\right)^{0.2}.$$

Versuchswerte für die Befeuchtungsraten sind angegeben für Wasser und Äthanol–Wasserfilme an senkrechten Oberflächen aus Kupfer, Stainless-steel, Perspex und Kohle. Der Einfluss unterschiedlicher Rohrlängen und Oberflächenrauhigkeiten wird im Temperaturbereich 20–50 °C untersucht bei Absorption von Äthanol–Luftgemischen durch die Filme. Effektive Oberflächenspannungen und Kontaktwinkel beim Stoffübergang wurden gemessen und mit Werten korreliert, die nach einer Methode für haftende Tropfen erhalten wurden. Die berechneten und gemessenen Werte für die Befeuchtungsraten, die zu stabilen Trockenzonen führen, stimmen für alle Oberflächen gut überein.

Аннотация—Рассматривается модель, объясняющая разрыв вертикальной ламинарной жидкой пленки под действием обратного потока растворимого газа. Условия, при которых вначале образуется стабильное сухое пятно, можно рассчитать из уравнения

$$\frac{\Gamma}{\mu} = 1{,}12(1 - \cos\theta)^{0.6}\left(\frac{\rho\gamma_e^3}{\mu^4 g}\right)^{0.2}$$

Приводятся экспериментальные данные для водяной и водно–этаноловой пленки на вертикальных графитовых, медных, стальных (нержавеющая сталь) и других трубчатых поверхностях. Изучается влияние различных длин трубки и шероховатости поверхности в температурном диапазоне 20–50°C в процессе поглощения плёнками воздушно–этаноловых смесей. Измеряются эффективные поверхностные натяжения и контактные углы в условиях массообмена и сопоставляются со значениями, полученными по капельному методу. Измеренные и расчетные значения параметров, определяющих образование стабильных пятен, для всех поверхностей находятся в хорошем согласии.